Algorithm Description Ver.1.1 (2016.12.19)
Algorithm Description Ver.1.2 (2019.3.31)
Algorithm Description Ver.2 (2020.3.31)

PI:Takafumi Hirata (GCOM-C/SGLI Ocean Team)
CI: Yohei Yamashita

Derivation of the absorption coefficient of Colourd Dissolved Organic Matter (CDOM)

1. Physics of the problem

The IOP algorithm assumes that the remote sensing reflectance (R_{rs}) *just above the sea surface* (denoted by z=0+, where z represents a depth), or the water-leaving reflectance (ρ), is obtained in prior to its implementation.

The R_{rs} for a wavelength λ is defined by

$$R_{rs}(\theta_v, \varphi_v, z=0+, \theta_s, \varphi_s, \lambda) = L_w(\theta_v, \varphi_v, z=0+, \theta_s, \varphi_s, \lambda) / E_d(z=0+, \theta_s, \varphi_s,\lambda) \quad (1)$$

where L_w and E_d are the radiance and the downward plane irradiance at the observation angle (zenith angle θ_v, azimuth angle, φ_v) and the solar angle (zenith angle θ_s, azimuth angle φ_s). The water-leaving reflectance ρ can be obtained by $\rho = \pi R_{rs}$. Morel and Gentili (1993, 1996) showed that the Eq. (1) can be related to the absorption coefficient a_t and the backscattering coefficient of the bulk water b_{bt} by

$$R_{rs} (\theta_v, \varphi_v, z=0+, \theta_s, \varphi_s, \lambda)= R (W, \theta_s, \varphi_s, \lambda) F(\theta_v, \varphi_v, z=0-, \theta_s, \varphi_s, \lambda) [b_{bt} (z=0-, \lambda)/a_t(z=0-, \lambda)] \quad (2)$$

where R is a transmittance from water to air and W denotes the wind speed. For convenience, all dependencies of the variables on illumination and observation geometries, depth, wavelength etc in Eq. 2 are omitted hereafter, unless otherwise specified. In addition, R x F will be denoted by F' so that Eq.2 is simplified by

$$R_{rs} = F' [b_{bt}/a_t]. \quad (3)$$

The absorption coefficient of the bulk seawater is decomposed into the absorption coefficients of optically active components. It is a common exercise to define those components as pure seawater (a_w) , phytoplankton (a_{ph}), non-algal particles NAP (a_d), and CDOM(a_g), so that

$$a_t=a_w+a_{ph}+a_{dg} \quad (4)$$

where

$a_{dg=}a_d+a_g$ $(a_d>0, a_g>0)$ (5)

Among the components, a_{ph} and $a_d+a_g(=a_{dg})$, thus not a_d and a_g, can be derived from the SGLI/GCOM-C1 IOP algorithm (see Smyth et al., 2006 as wel as ATBD for the IOP algorithm). Hence, we assume that a_{dg} are known in this document. A practical problem here is to decompose a_{dg} into a_d and a_g to retrieve a_g.

2. Dataset

A global in situ dataset was used (Werdell and Bailey 2005) to derive a_g from a_{dg}. Figure 1 shows the data distribution of the dataset.

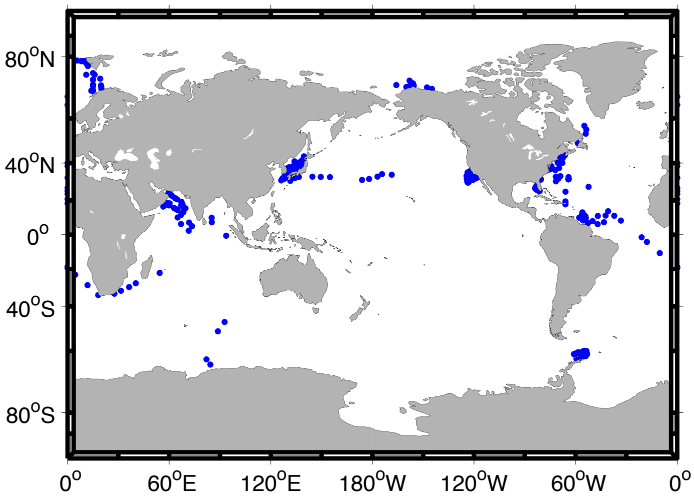

Figure 1 NOMAD data distribution

3. Algorithm

The CDOM algorithm here takes the a_{dg} as an input. Thus, the algorithm decomposes a_{dg} into a_g and a_d in practice. Since the IOP algorithm retrieves a_{dg} relatively well at shorter wavelengths than other longer wavelengths (Smyth et al., 2006), the former wavelengths will be considered below to derive a_g. Considering that (i) an optical separation of a_g from a_{dg} is challenging as they often have a similar spectrum (IOCCG, 2018) and (ii) a_{dg} derived from the IOP model would in practice include some uncertainty anyway so that a fuzzy algorithm which can accepts input error may be desired , our choice is to derive a_g from a_{dg} using an empirical (or statistical) relationship between a_g and a_{dg} rather than using an optical theory: the statistical coefficients can wrap up the above-mentioned uncertainty while bypassing the theoretical challenge. Figure 2 show the empirical relationship between a_g and a_{dg} for 412nm obtained from the in situ data. While the simple statistical model of a_g=s*$(a_{dg})^k$ (i.e. a linear regression model in log-log scale) shows a better r^2, it also exceeds 1:1 line at smaller end of a_{dg} so that $a_g > a_{dg}$ (see a circle in Figure 2). When satellite-derived a_{dg} is even smaller than the smallest a_{dg} found in the present in situ dataset (which is likely to happen because a satellite data usually covers a larger spatial domain than in situ observation), a resultant a_g derived from the fit would violate Eq. 5. Hence, we employ the other statistical model that never exceeds 1:1 line:

$$a_g(411) = \frac{A*a_{dg}(411)}{B+C*a_{dg}(411)} + D \tag{6}$$

where A=1.5625, B=1.7647, C=0.6058 and D=-0.0007218 which are determined by the least square fit. Although Eq. 6 reduces r^2 statistics by 0.07 (i.e. data variance of 7% is less explained) when compared to the a_g=s*$(a_{dg})^k$, also shows a better fit at the higher end of a_{dg} than $_g$=s*$(a_{dg})^k$ (squared area in Figure 2).

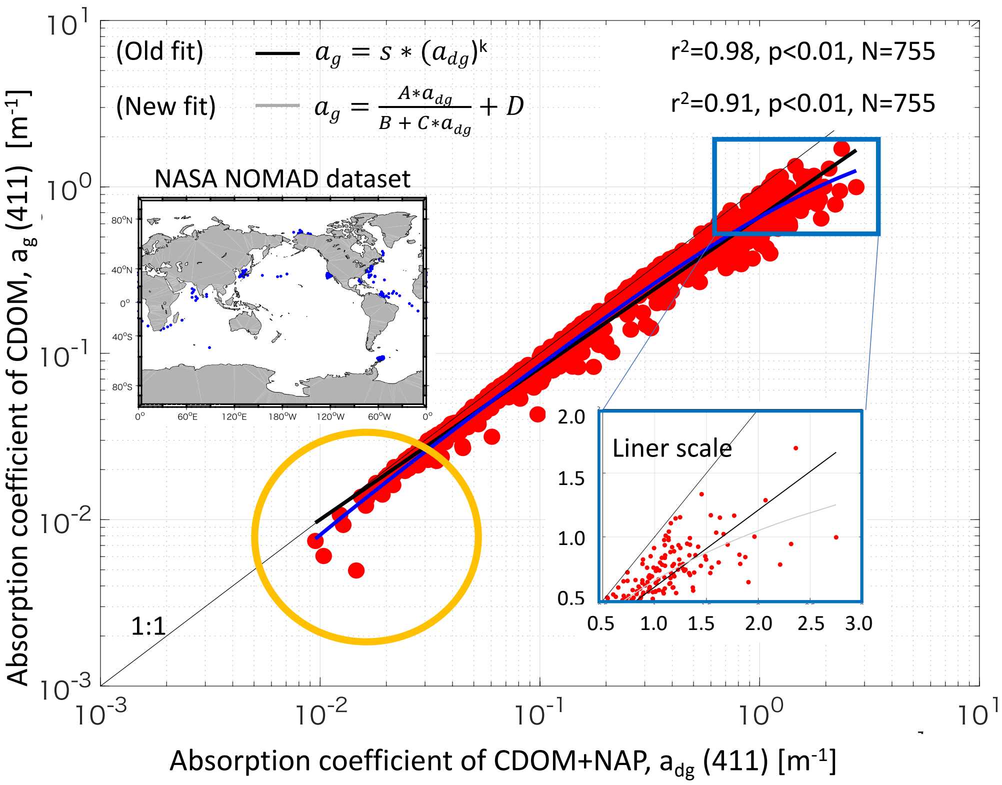

Figure 2. In situ relationship between a_g (412) and a_{dg} (411).

Note that Eq. 6 (with the coefficient values mentioned above) leads to a_g=-0.0007218 < 0, when a_{dg}=0. Although this also does not make sense, the value of $a_g(412)$=-0.0007218 is either lower than detection limit of an instrument or within an uncertainty of the measurement.

Using the actual SGLI/GCOM-C satellite data, a_g was derived and matched up with a_g measured in situ (Table 1). Match up was made in such a way that satellite data do not deviate more than +/- 3 hours from the in situ observation time. A 3x3 satellite pixel window is selected (Werdell and Bailey, 2005) so that a pixel nearest to the exact latitude and longitude of an in situ measurement is located at the center of the window, and an average of a_g within the window is calculated to represent the satellite a_g. Then the satellite a_g is compared to the a_g measured in situ. Although statistical conclusion cannot be drawn due to a lack of a sufficient number of measurements, the differences between the satellite- and in situ a_g (in linear scale) are between -89.2% and +98.3%.

Table 1

In situ data credit: Profs. Yamashita/Suzuki

$a_{CDOM}(412)$ $[m^{-1}]$	Date	Latitude	Longitude	Satellite Data (250m/pixel) 3x3 pixels average	In Situ Data	Difference [%]
Old fit	2018.5.27	35.83 ° N	144.00 ° E	0.0294	0.0471	-37.6%
New fit	2018.5.27	35.83 ° N	144.00 ° E	0.0156	0.0471	-66.9.%
					In situ data credit: Prof. Isada	
Old fit	2018.6.01	45.52 ° N	142.12 ° E	0.1641	0.0633	+159.3%
New fit	2018.6.01	45.52 ° N	142.12 ° E	0.1256	0.0633	+98.3%
					In situ data credit: Prof. Isada	
Old fit	2018.6.03	45.41 ° N	145.16 ° E	0.0922	0.0922	+58.3%
New fit	2018.6.03	45.41 ° N	145.16 ° E	0.1110	0.0922	+20.3 %
					In situ data credit: Prof. Ishizaka	
Old fit	2018.7.20	31.75 ° N	128.16 ° E	0.0253	0.0818	-69.1 %
New fit	2018.7.20	31.75 ° N	128.16 ° E	0.0162	0.0818	-89.2%

Reference:

Smyth, T. J., G.F. Moore, T. Hirata, J. Aiken, Semianalytical model for the derviation of ocean colour inherent optical properties: description, implementation, and performance assessment, Applied Optics, 45, 8116-8131, 2006.

Werdell, P. J. and S. W. Bailey, An improved in situ data set for bio-optical algorithm development and ocean color satellite validation, Remote Sens. Environ., 98, 122-140, 2005